

Symmetry of high-piezoelectric Pb based complex perovskites at the morphotropic phase boundary II. Theoretical treatment

Yasusada YAMADA^{1,2,*}, Yoshiaki UESU^{1,3}, Masaaki MATSUDA², Kouji FUJISHIRO⁴, Dave E. COX⁵, Beatriz NOHEDA⁵ and Gen SHIRANE⁵

¹Advanced Research Institute, Waseda University, 3-4-1 Okubo, Shinjuku-ku, Tokyo 169- 8555

²Advanced Science Research Center, Japan Atomic Energy Research Institute, Tokai, Ibaraki 319- 1195

³Department of Physics, Waseda University, 3-4-1 Okubo, Shinjuku-ku, Tokyo 169- 8555

⁴Materials and Structures Laboratory, Tokyo Institute of Technology, 4259 Nagatsuda, Midori-ku, Yokohama 226- 8503

⁵Department of Physics, Brookhaven National Laboratory, Upton, New York 11973

(Received November 5, 2018)

The structural characteristics of the perovskite-based ferroelectric $\text{Pb}(\text{Zn}_{1/3}\text{Nb}_{2/3})_{1-x}\text{Ti}_x\text{O}_3$ at the morphotropic phase boundary (MPB) region ($x \simeq 0.09$) have been analyzed. The analysis is based on the symmetry adapted free energy functions under the assumption that the total polarization and the unit cell volume are conserved during the transformations between various morphotropic phases. Overall features of the relationships between the observed lattice constants at various conditions have been consistently explained. The origin of the anomalous physical properties at MPB is discussed.

KEYWORDS: Piezoelectricity, morphotropic phase boundary, neutron diffraction, $\text{Pb}(\text{Zn}_{1/3}\text{Nb}_{2/3})\text{O}_3/9\%\text{PbTiO}_3$

§1. Introduction

The physical properties in solids at the phase boundaries between the two competitive stable phases tend to exhibit anomalous characteristics. A typical example is seen in the extraordinary transport phenomena such as high- T_c superconductivity and colossal magnetoresistance at metal-insulator phase boundary of the transition metal oxides. The high piezoelectric effect at the morphotropic phase boundary (MPB) observed in several perovskite-based ferroelectric materials may be considered to provide another interesting example of such phenomena at the structural phase boundary.

As is discussed in Part I¹⁾ of the present paper, the high piezoelectricity has been investigated from both experimental as well as theoretical aspects. Experimentally, Noheda *et al.*²⁻⁵⁾ discovered a previously unknown monoclinic phase belonging to space group Cm (M_a -phase) in the boundary region between rhombohedral (R) and tetragonal phases in $\text{Pb}_1\text{Zr}_{1-x}\text{Ti}_x\text{O}_3$ (abbreviated as PZTx). This is immediately followed by the theoretical work by Bellaiche *et al.*⁶⁾ Based on the first principles calculations they showed that there should in fact exist M_a -phase within a narrow concentration range intervening between the high symmetry R- and T- phase in PZTx system in complete agreement with the experimental results. It is also pointed out that the high piezoelectricity is associated with the stabilization of the monoclinic phase.

Subsequently, X-ray measurements by Noheda *et al.*⁷⁾ on another type of material $\text{Pb}(\text{Zn}_{1/3}\text{Nb}_{2/3})_{1-x}\text{Ti}_x\text{O}_3$ (abbreviated as PZN-xPT) also revealed the existence of

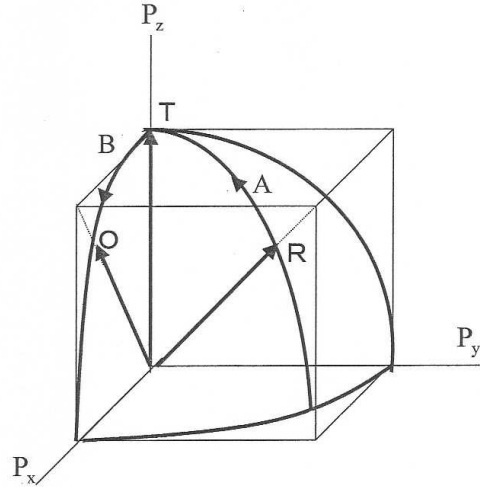


Fig. 1. The trajectory followed by \mathbf{P}_s in the 3-dimensional polarization vector space. R, T and O represent the symmetries of the structure as \mathbf{P}_s is oriented to $[111]$, $[001]$, and $[101]$ respectively. The symbols A and B indicate the process between $\text{R} \rightarrow \text{T}$ and $\text{T} \rightarrow \text{R}$ respectively.

similar monoclinic phase at the MPB region, except that the space group in this case is Pm (M_c -phase) instead of Cm .

On the other hand, Ishibashi and Iwata⁸⁻¹⁰⁾ developed a phenomenological theory on the physical properties at morphotropic phase boundary in perovskite solid solutions. He pointed out that depending on the coefficients of fourth order terms of the free energy expansion, the system stabilizes the orthorhombic phase intervening between the tetragonal and the rhombohedral phases. He

* E-mail: yasusada@mn.waseda.ac.jp

also discussed the dielectric^{8,9)} as well as elastic¹⁰⁾ responses of the system at MPB and pointed out that the anomalous behavior in the susceptibility tensor components is in fact due to large electromechanical coupling constants of these materials. Fu and Cohen¹¹⁾ presented the key concept to understand the physics of high piezoelectricity: that is, the rotation of the spontaneous polarization during the structural transitions under electric field. Through first principles calculations they showed that there is a low energy path along the lines combining the symmetric directions of [111], [001] and [101] as shown in Fig.1. Upon application of the external field, the polarization would easily rotate along the particular path, which results in a large piezoelectric response. The stabilization of the monoclinic phase are considered to manifest this view point since monoclinicity is induced during the polarization vector continuously rotates along the specific path.

As is discussed by Noheda *et al.*,⁷⁾ in the case of PZN-8PT, the M_c -phase appears on the path between $\mathbf{P} \parallel [001]$ and $\mathbf{P} \parallel [101]$. This suggests that the high symmetry stable phase for composition around 8PT would be tetragonal and orthorhombic (O) rather than rhombohedral. In fact, depending on the prehistory of the sample preparation such as heat treatment, poling, etc., the orthorhombic phase is observed to become stabilized in PZN-9PT powder sample.¹²⁾

Recently, we carried out a neutron diffraction study using single crystals of PZN-9PT, with focus on the existence of M_c -phase. The results are summarized in Part I of the present paper. In the present study, we develop a theoretical treatment based on a phenomenological arguments in order to analyze the experimental results presented in Part I. Since the treatment is phenomenological, unlike the treatment based on the first principles calculations, the conclusions depend on a few disposable parameters included in the free energy expression. Nevertheless, the results seem to provide some important insights into the specific physics at MPB regions.

§2. Analysis of Experimental Data

Using BaTiO₃ as a model system, Fu and Cohen¹¹⁾ developed a detailed theoretical treatment and discussed that the morphotropic phase transition scheme in BaTiO₃ is described by the 'rotation' of the spontaneous polarization vector, \mathbf{P}_s , within the (P_x, P_y, P_z) space moving along [111]→[001]→[101] directions as shown in Fig. 1. This process realizes the phases with rhombohedral, tetragonal and orthorhombic symmetry. Later, Vanderbilt and Cohen¹³⁾ pointed out that when the energy terms up to the eighth order with respect to polarization are included in the free energy expansion, the monoclinic phases with the polarization along $[\xi \ \xi \ \zeta]$ -(M_a -phase) and $[\xi \ 0 \ \zeta]$ -(M_c -phase) directions can be stabilized.

Following these previous arguments, we also assume that the polarization moves on the surface of the sphere with $|\mathbf{P}_s|$ conserved during the process of the polymorphic phase transitions in the present system. For later convenience, let us define the parameters to specify the orientation of polarization as it moves along the trajec-

tories A and B in the \mathbf{P} -space (See Fig.1.) as follows:
process A:

$$\rho = \frac{P_z^2}{P^2}, \quad (2.1)$$

process B:

$$\rho' = \frac{P_x^2}{P^2}, \quad (2.2)$$

In the process A, ρ changes in the range of $\frac{1}{3} \leq \rho \leq 1$ as \mathbf{P} rotates from [111] ($\rho = \frac{1}{3}$) to [001] ($\rho = 1$), while in the process B, ρ' changes in the range of $0 \leq \rho' \leq \frac{1}{2}$ as \mathbf{P} rotates from [001] ($\rho' = 0$) to [101] ($\rho' = \frac{1}{2}$).

In addition, we further assume that the volume of the unit cell is also conserved throughout the sequential phase transitions. As is typically seen in the case of BaTiO₃, this assumption seems to be satisfied well.

Since we are particularly interested in the lattice distortions, we give the expression of the 'elastic' free energy leaving the strain components as the independent variables rather than projecting on the polarization space. In order to make the treatment physically transparent, we construct the basis functions of the six dimensional direct product space of $(P_x^2, P_y^2, P_z^2, P_y P_z, P_z P_x, P_x P_y)$ and $(e_{xx}, e_{yy}, e_{zz}, e_{yz}, e_{zx}, e_{xy})$ associated with the irreducible representations of the point group $m\bar{3}m$ as follows.

$$\begin{aligned} \psi_1 &= \frac{1}{\sqrt{3}}(P_x^2 + P_y^2 + P_z^2) \in A_{1g} \\ \psi_2 &= \frac{1}{\sqrt{6}}(2P_z^2 - P_x^2 - P_y^2) \\ \psi_3 &= \frac{1}{\sqrt{2}}(P_x^2 - P_y^2) \end{aligned} \left. \vphantom{\begin{aligned} \psi_1 \\ \psi_2 \\ \psi_3 \end{aligned}} \right\} \in E_g$$

$$\begin{aligned} \psi_4 &= P_y P_z \\ \psi_5 &= P_z P_x \\ \psi_6 &= P_x P_y \end{aligned} \left. \vphantom{\begin{aligned} \psi_4 \\ \psi_5 \\ \psi_6 \end{aligned}} \right\} \in T_{2g} \quad (2.3)$$

and

$$\begin{aligned} e_1 &= \frac{1}{\sqrt{3}}(e_{xx} + e_{yy} + e_{zz}) \in A_{1g} \\ e_2 &= \frac{1}{\sqrt{6}}(2e_{zz} - e_{xx} - e_{yy}) \\ e_3 &= \frac{1}{\sqrt{2}}(e_{xx} - e_{yy}) \end{aligned} \left. \vphantom{\begin{aligned} e_1 \\ e_2 \\ e_3 \end{aligned}} \right\} \in E_g$$

$$\begin{aligned} e_4 &= e_{yz} \\ e_5 &= e_{zx} \\ e_6 &= e_{xy} \end{aligned} \left. \vphantom{\begin{aligned} e_4 \\ e_5 \\ e_6 \end{aligned}} \right\} \in T_{2g} \quad (2.4)$$

Then, we can set up the simplest symmetry adapted elastic free energy including only the quadratic (or bilinear) terms as follows:

$$F_{el} = F_{el}^{(A_{1g})} + F_{el}^{(E_g)} + F_{el}^{(T_{2g})}, \quad (2.5)$$

where

$$F_{el}^{(A_{1g})} = \frac{1}{2} c e_1^2 - g e_1 \psi_1, \quad (2.6)$$

$$F_{el}^{(E_g)} = \frac{1}{2} c' (e_2^2 + e_3^2) - g' (e_2 \psi_2 + e_3 \psi_3), \quad (2.7)$$

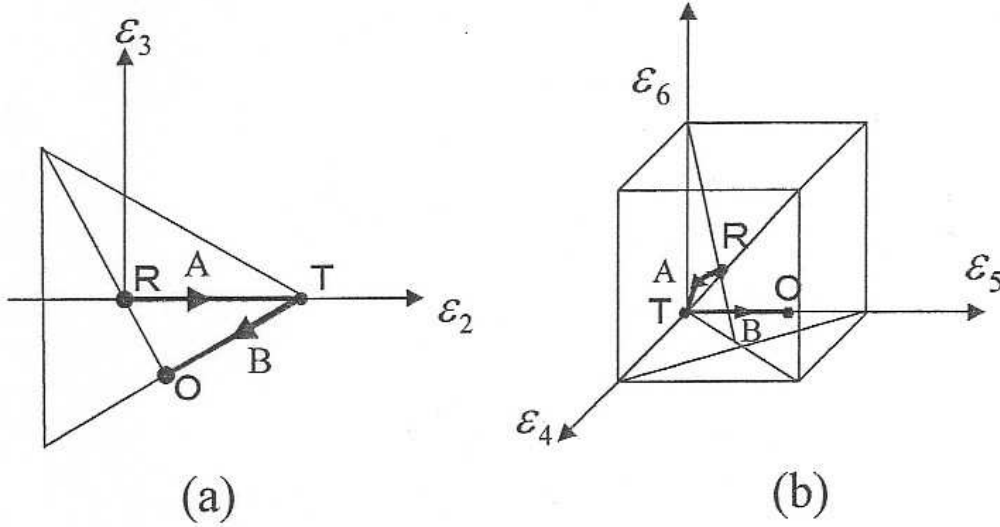


Fig. 2. (a) The trajectory followed by the lattice distortions in the 2-dimensional space spanned by the basis of E_g irreducible representation. (b) The trajectory followed by the lattice distortions in the 3-dimensional space spanned by the basis of T_{2g} irreducible representation.

$$F_{el}^{(T_{2g})} = \frac{1}{2}c''(e_4^2 + e_5^2 + e_6^2) - g''(e_4\psi_4 + e_5\psi_5 + e_6\psi_6). \quad (2.8)$$

The second terms of these equations give the electrostrictive energies in the cubic perovskite system.

In these expressions, the independent thermodynamical variables are e'_v s ($v = 1, \dots, 6$) while ψ'_v s are considered to be the parameters to define the orientation of the polarization which are explicitly given by ρ and ρ' in eqs. (2.1) and (2.2). Among the three terms in eq. (2.5), $F_{el}^{(A_{1g})}$ is irrelevant to determine the stability of the system during the rotation of the polarization vector, since it is expressed in terms of e_1 and ψ_1 which are both assumed to be conserved.

Moreover, $F_{el}^{(E_g)}$ is defined in the 2-dimensional space spanned by the basis of E_g representation (ϵ_2 and ϵ_3), while $F_{el}^{(T_{2g})}$ in the 3-dimensional space spanned by the basis of T_{2g} representation (ϵ_4, ϵ_5 , and ϵ_6). Therefore, in order to find the stable lattice distortions, we simply minimize $F_{el}^{(E_g)}$ and $F_{el}^{(T_{2g})}$ independently.

(i) E_g -space

By the standard minimization procedure, it is easily shown that the trajectory of the minimum energy $\epsilon^0(\rho)$ is given by:

(a) Process A

$$\left. \begin{aligned} \epsilon_2^0(\rho) &= \frac{g'}{\sqrt{6}c'}(3\rho - 1), \\ \epsilon_3^0 &= 0. \end{aligned} \right\} \quad (2.9)$$

(b) Process B

$$\left. \begin{aligned} \epsilon_2^0(\rho) &= \frac{g'}{\sqrt{2}c'}(1 - 2\rho'), \\ \epsilon_3^0 &= \frac{-2g}{\sqrt{6}c'}. \end{aligned} \right\} \quad (2.10)$$

where $\hat{\epsilon}_2$ and $\hat{\epsilon}_3$ are defined by 120° rotation of the (ϵ_2, ϵ_3) coordinate system.

The trajectory followed by the representative point of the system in the (ϵ_2, ϵ_3) space is given in Fig.2(a). In the figure, R, T and O represents the rhombohedral, tetragonal and orthorhombic phases respectively.

(ii) T_{2g} -space

Similarly, we have the trajectory of the energy minimum path:

(a) Process A

$$\left. \begin{aligned} \epsilon_4^0(\rho) &= \epsilon_5^0(\rho) = \frac{g''}{c''}\sqrt{\frac{\rho(1-\rho)}{2}}, \\ \epsilon_6^0(\rho) &= \frac{g''}{c''}\frac{1-\rho}{2}. \end{aligned} \right\} \quad (2.11)$$

(b) Process B

$$\left. \begin{aligned} \epsilon_4^0 &= \epsilon_6^0 = 0, \\ \epsilon_5^0(\rho') &= \frac{g''}{c''}\sqrt{\rho'(1-\rho')}. \end{aligned} \right\} \quad (2.12)$$

The trajectories followed by the representative point of the system in the $(\epsilon_4, \epsilon_5, \epsilon_6)$ space is given in Fig.2(b).

Eqs. (2.9) to (2.12), together with the condition of the volume conservation ($\epsilon_{xx}^0 + \epsilon_{yy}^0 + \epsilon_{zz}^0 = 0$), give the set of lattice parameters of the stable state in terms of ρ or ρ' as shown in Table I. Notice among total of 30 lattice constants, there are only two disposable parameters, Δ and δ , besides ρ and ρ' . We utilized the values of c_1 (the unique axis in T-phase) observed in 9PT5 and β (monoclinic angle in O-phase) in 9PT4 as tabulated in Part I

Table I. The lattice distortions of the perovskite system in the polymorphic phases realized when \mathbf{P}_s rotates through the process A and B. The disposable parameters are defined by: $\Delta = \frac{2g'}{3c'}$, $\delta = \frac{g''}{3c''}$.

| | ρ | ρ' | ε_{xx} Δa | ε_{yy} Δb | ε_{zz} Δc | ε_{yz} $\Delta\alpha$ | ε_{zx} $\Delta\beta$ | ε_{xy} $\Delta\gamma$ |
|----------------|---------------|---------------|----------------------------------|----------------------------------|----------------------------------|--|--|--------------------------------------|
| R | $\frac{1}{3}$ | | 0 | 0 | 0 | δ | δ | δ |
| M _a | ρ | - | $-\frac{(3\rho-1)\Delta}{4}$ | $-\frac{(3\rho-1)\Delta}{4}$ | $+\frac{(3\rho-1)\Delta}{2}$ | $3\delta\sqrt{\frac{\rho(1-\rho)}{2}}$ | $3\delta\sqrt{\frac{\rho(1-\rho)}{2}}$ | $3\delta\frac{(1-\rho)}{2}$ |
| T | 1 | 0 | $-\frac{\Delta}{2}$ | $-\frac{\Delta}{2}$ | Δ | 0 | 0 | 0 |
| M _c | - | ρ' | $\frac{(-1+3\rho')\Delta}{2}$ | $-\frac{\Delta}{2}$ | $\frac{(2-3\rho')\Delta}{2}$ | 0 | $3\delta\sqrt{\rho'(1-\rho')}$ | 0 |
| O | - | $\frac{1}{2}$ | $\frac{\Delta}{4}$ | $-\frac{\Delta}{2}$ | $\frac{\Delta}{4}$ | 0 | $\frac{3}{2}\delta$ | 0 |

(see Table I) to obtain the value of Δ and δ respectively.

Fig.3 shows the sequence of the calculated lattice constants to be taken by the system as ρ and ρ' is varied to stabilize (R)→(M_a)→T→M_c→O, including the fictitious stable phases R and M_a which are not realized in the PZN-9PT system, but realized in the related materials. The observed values at lower temperatures given in Part I are indicated by the solid circles. We can not calculate the lattice parameters as a function of temperature for direct comparison with the experimental results, since the temperature dependences of $\rho(T)$ and $\rho'(T)$ are outside of the framework of the present treatment.

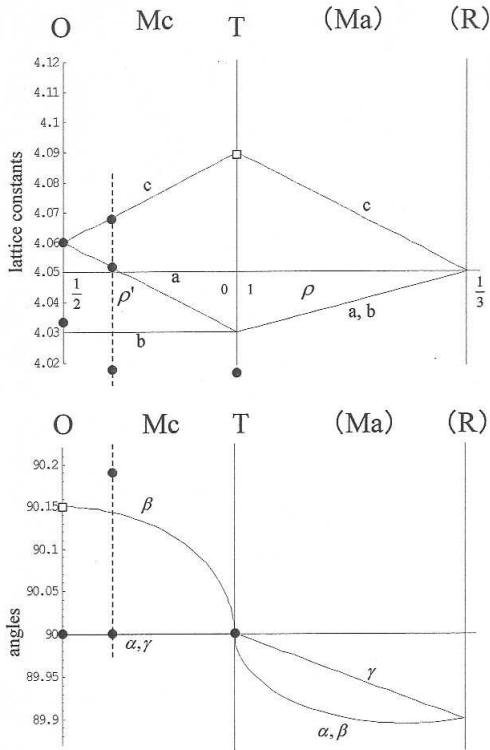


Fig. 3. The calculated variation of the lattice constants in PZN-9PT as the parameters ρ and ρ' is varied. The solid circles are the experimental values obtained by the present work (Part I). The figure includes the fictitious phases (R and M_a) which are not realized in 9PT, but realized in the closely related systems. The open squares indicate the data used for the numerical analysis. (See the Text.)

§3. Conclusions and Discussions

In conclusion, based on the symmetry adapted free energy function, we analyze the structural characteristics of PZN-9PT under the assumption that the total polarization and the unit cell volume are conserved during the transformations between various morphotropic phases. Overall features of the relationship between the observed lattice constants in various phases have been consistently explained.

So far, we have discussed the lattice distortions which are directly observed by the diffraction studies described in Part I. The energetic considerations concerning the stability of the phases seem to give more important insight into the physical properties of the system at MPB as discussed in the following.

Using eqs. (2.9) through (2.12), the free energy values of the rhombohedral ($F_{el}(R)$), the tetragonal- ($F_{el}(T)$), and the orthorhombic- ($F_{el}(O)$) phases are given by,

$$\left. \begin{aligned} F_{el}(R) &= -\frac{g''^2}{6c''^2}, \\ F_{el}(T) &= -\frac{g'^2}{3c'^2}, \\ F_{el}(O) &= -\frac{g'^2}{12c'^2} - \frac{g''^2}{8c''^2}, \end{aligned} \right\} \quad (3.1)$$

which means that ($F_{el}(O)$) is expressed by a fixed weighted mean of ($F_{el}(R)$) and ($F_{el}(T)$) as,

$$F_{el}(O) = \frac{1}{4} F_{el}(T) + \frac{3}{4} F_{el}(R), \quad (3.2)$$

irrespective of the parameter values of c 's and g 's. Assuming, for simplicity, linear dependence of the parameters on the x -value (the concentration of PbTiO₃), the relative energies of the three phases change with respect to x as schematically shown in Fig.4. We see that the stable phases are generally given by either T- or R- phases while O-phase barely becomes one of the three degenerated ground states at the single critical concentration, x_c , where,

$$\frac{g'^2}{3c'^2} = \frac{g''^2}{6c''^2} \equiv A \quad (3.3)$$

is satisfied. Notice the critical concentration $x = x_c$ is nothing but the MPB point. (See Fig.4.)

More generally, the free energy $F_{el}(\rho)$ and $F_{el}(\rho')$ with

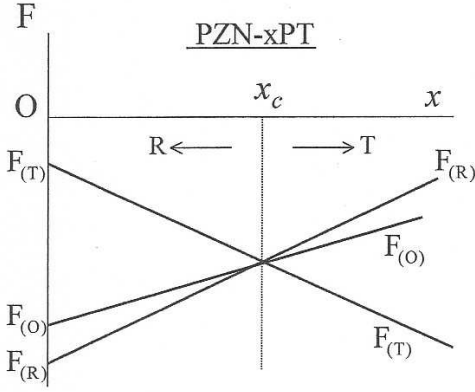


Fig. 4. Schematic diagram of the relative phase stability as x -value (the concentration of PbTiO_3) is changed. The orthorhombic phase is stable only at the single critical concentration, x_c , which just corresponds to MPB point.

an arbitrary polarization direction is given by,

$$F_{el}(\rho) = -\frac{g'^2}{12c'}(3\rho - 1)^2 - \frac{g''^2}{8c''}(1 - \rho)(1 + 3\rho), \quad (3.4)$$

$$F_{el}(\rho') = -\frac{g'^2}{12c'} - \frac{g'^2}{4c'}(1 - 2\rho')^2 - \frac{g''^2}{2c''}\rho'(1 - \rho'). \quad (3.5)$$

It is easily seen that at MPB where eq. (3.3) is satisfied,

$$F_{el}(\rho) = F_{el}(\rho') = A, \quad (3.6)$$

irrespective of the values of ρ and ρ' which means that at MPB, the energy is completely degenerated throughout the postulated path of polarization rotation. Only by the introduction of higher order energy terms which are neglected in the present treatment, the degeneracy will be lifted so that either of O-, M_a - or M_c - phases may become stabilized in the MPB region as shown by Vanderbilt and Cohen.¹³⁾ This situation may explain the experimental observations that depending on subtle differences of the prehistory of sample preparation, the symmetry of the stable state becomes different.

Furthermore, neglecting the higher order terms, we see that at $x = x_c$ the system could move over between $R \rightleftharpoons M_a \rightleftharpoons T \rightleftharpoons M_c \rightleftharpoons O$ under external forces such as electric field and stress without any cost of elastic energy. Therefore, at MPB some of the susceptibility tensor components of χ_{ij} (dielectric constants), d_{ijk} (piezoelectric constants) and the inverse of c_{ijkl} (elastic constants) should critically blow up, although in the real system, the higher order effects would tend to prevent such a strong anomaly. Actually, Ishibashi and Iwata⁸⁻¹⁰⁾ have given the explicit expressions for these susceptibility tensors, some of which tend to show the critical behavior. The above simple energy considerations seem to reveal the essential origin of the anomalous physical properties

at MPB.

As a further application of this view point, we take notice on the elastic anomaly exhibited by hexagonal BaTiO_3 .¹⁴⁾ It is known that hexagonal BaTiO_3 (h-BT) undergoes two phase transitions successively as hexagonal \rightarrow orthorhombic (space group $C222_1$) \rightarrow monoclinic (space group $P2_1$).^{15,16)} The relevant order parameter is the doubly degenerated phonon modes, Q_1 and Q_2 . Ishibashi^{17,18)} pointed out that the transition between O- and M- phases is caused by the rotation of the polarization vector of the mode in the 2-dimensional (Q_1, Q_2)-space, which is very similar to the feature presented in this paper if we replace \mathbf{P} by \mathbf{Q} . However, it should be noticed that the anomaly at the O-M transition region in h-BT is manifested in the elastic compliances rather than piezoelectricity because the \mathbf{Q} -modes are optically inactive. In this context, h-BT may be considered to provide another example belonging to the different category concerning MPB adventure.

Acknowledgements

Financial supports of Grant-In-Aid for Science Research from Monbu-Kagakusho, Grant for Development of New Technology from Shigaku-Shinkozaidan, Waseda University Grant for Special Research Projects and US DOE under contract No.DE-AC0298CH10866 are also gratefully acknowledged. This work was performed under US-Japan Cooperative Neutron Research Program.

- 1) Y. Uesu, M. Matsuda, Y. Yamada, K. Fujishiro, D. E. Cox, B. Noheda and G. Shirane: This issue.
- 2) B. Noheda, D. E. Cox, G. Shirane, E. Cross and S-E. Park: Appl. Phys. Lett. **74** (1999) 2059.
- 3) B. Noheda, J. A. Gonzalo, E. Cross, R. Guo, S-E. Park, D. E. Cox and G. Shirane: Phys. Rev. **B61** (1999) 8687.
- 4) R. Guo, E. Cross, S-E. Park, B. Noheda, D. E. Cox and G. Shirane: Phys. Rev. Lett. **84** (2000) 5423.
- 5) B. Noheda, D. E. Cox, G. Shirane, R. Guo, B. Jones and E. Cross: Phys. Rev. **B63** (2001) 14103.
- 6) L. Bellaiche, A. Garcia and D. Vanderbilt: Phys. Rev. Lett. **84** (2000) 5427.
- 7) B. Noheda, D. E. Cox, G. Shirane, S-E. Park, E. Cross and Z. Zhong: Phys. Rev. Lett. **86** (2001) 3891.
- 8) Y. Ishibashi and M. Iwata: Jpn. J. Appl. Phys. **37** (1998) L985.
- 9) Y. Ishibashi and M. Iwata: Jpn. J. Appl. Phys. **38** (1999) 800.
- 10) Y. Ishibashi and M. Iwata: Jpn. J. Appl. Phys. **38** (1999) 1454.
- 11) H. Fu and R. E. Cohen: Nature **403** (2000) 281.
- 12) D. E. Cox, B. Noheda, G. Shirane, Y. Uesu, K. Fujishiro and Y. Yamada: Appl. Phys. Lett. (9th issue of July, 2001 in press).
- 13) D. Vanderbilt and M. H. Cohen: Phys. Rev. **B63** (2001) 094108.
- 14) M. Yamaguchi, K. Inoue, T. Yagi and Y. Akishige: Phys. Rev. Lett. **74** (1995) 2126.
- 15) E. Sawaguchi, Y. Akishige and T. Yamamoto: Ferroelectrics **106** (1990) 63.
- 16) K. Inoue, A. Hasegawa, K. Watanabe, H. Uwe and T. Sakudo: Phys. Rev. **B38** (1998) 6352.
- 17) Y. Ishibashi and M. Tomatsu: J. Phys. Soc. Japan **58** (1989) 1058.
- 18) Y. Ishibashi: J. Phys. Soc. Japan **63** (1994) 1396.